Parvalbumin interneuron dendrites enhance gamma oscillations: some technical additions

Birgit Kriener[1,*], Hua Hu[1], and Koen Vervaeke[1]

[1]Institute of Basic Medical Sciences, University of Oslo, Norway.
[*]Correspondence: bhekriener@gmail.com

Connectivity statistics of ring and two-dimensional networks

In the section "METHOD DETAILS: Network models" in the STAR METHODS we introduced the network model we generally used in the paper, the choice motivated by one of the most prominent models for studying biophysically constrained gamma-oscillations [Bartos et al., 2002, Vida et al., 2006]. In some simulations (Suppl. Fig. 5A-C) however, we also simulated networks constrained by recent connectivity statistics data measured in simultaneous patch-clamp recordings of PV basket cells [Espinoza et al., 2018], see section "METHOD DETAILS: Network models, Two-dimensional PV basket cell network". These networks differ from ring networks in several ways. First, the connection probabilities are quite different, especially with respect to the spatial reach, see Suppl. Fig. 5A,B. Second, the density of cells as a function of distance differs in one-dimensional ring networks and two-dimensional torus networks. This will have pronounced impact on the number of connections at any given distance, and also on the delay distribution and, hence, timing of incoming spikes. This makes a direct comparison difficult.

In this technical section we will quantitatively analyze these differences in formal detail and discuss our choice to match the compound inhibitory conductance $G_{GABA}(t)$ each neuron would receive given total synchrony in both networks. This choice allows us to directly relate results for the two networks with an emphasis on topology.

Ring networks

The standard network setting is derived from the networks considered in [Bartos et al., 2002, Vida et al., 2006], with N neurons arranged equidistally on a ring. Connectivity was established randomly following a Gaussian connection probability

$$p_{\text{ring}}(d) = e^{-d^2/2\sigma^2}\Theta[d_{\max} - d],\ d_{\max} = \left\lfloor \frac{N}{4} \right\rfloor , \tag{1}$$

with Heaviside step-function $\Theta[x] = 0$ if $x < 0$, $\Theta[x] = 1$ otherwise, and floor-operator $\lfloor x \rfloor$ that rounds x to the next lowest integer. The standard deviation was chosen $\sigma = 24$ neuron distances [Bartos et al., 2002, Vida et al., 2006]. Autapses were usually excluded, and test network runs

including autapses did not show any palpable differences (not shown). In a ring network neuron density is discrete, but constant with distance, i.e.,

$$\rho_{\text{ring}}(d) = \frac{N}{L}\delta(d_i - d)\Theta\left[d_{\max} - d\right], \quad d_i \in \mathbb{Z} \setminus 0, d_{\max} = \left\lfloor \frac{N}{4} \right\rfloor \tag{2}$$

with Dirac measure $\delta(x) = 1$ if $x = 0$, and zero otherwise. Hence the probability mass function of distances $f(d)$ (see Fig. 1A) is given by

$$f_{\text{ring}}(d) = \frac{\rho_{\text{ring}}(d)p_{\text{ring}}(d)}{\int_{d=0}^{d_{\max}} \rho_{\text{ring}}(x)p_{\text{ring}}(x)\,dx}, \tag{3}$$

where the denominator yields the expected number of connected neurons per neuron $\langle k \rangle$,

$$\begin{aligned} \langle k_{\text{ring}} \rangle &= \int_{d=0}^{d_{\max}} \rho_{\text{ring}}(x)p_{\text{ring}}(x)\,dx \\ &= \sum_{d_i=-N/4, d_i\neq 0}^{N/4} \frac{N}{2L} e^{-d_i^2/2\sigma^2} \approx \frac{\sqrt{\pi}N\sigma}{2\sqrt{2}L}\,\text{erf}\left(\frac{L}{\sqrt{2\sigma}}\right) \approx 58\,. \end{aligned} \tag{4}$$

If two neurons were connected, a total number of $n_{\text{syn}} = \lfloor n_{\max} p(d) \rfloor$ ($n_{\max} = 6$, so $\max(n_{\text{syn}}) = 5$ in absence of autapses) GABAergic synapses were randomly distributed across a perisomatic region including the soma (with probability $1/3$) and dendrites (with probability $2/3$) upto $50\,\mu$m from the the somatic center. This yielded an average number of synapses $\langle n_{\text{syn}} \rangle \approx 3.7$ between any two connected neurons.

The distance-dependent total conductance $n_{\text{syn}}(d) \times \bar{g}$ between any two neurons (also known as unitary conductance) is plotted in Fig. 1B,C for three different synaptic strengths in absolute and relative (to cell membrane area) terms, respectively.

The spike transmission delay τ is a linear function of the distance, i.e.,

$$\tau(d) = \tau_0 + v_c d\,. \tag{5}$$

The constant offset τ_0 represents a synaptic delay, while the distance dependent delay is a conduction delay that represents the finite velocity v_c of action potential propagation along the axon. The resulting probability mass function $f_{\text{ring}}(\tau)$ of delays is given by (see Fig. 1E)

$$\tau_0 + f_{\text{ring}}(\tau) = \tau_0 + \frac{e^{\tau^2/2\sigma_\tau^2}}{\sum_{\tau=\tau_{\min}}^{\tau_{\max}} e^{\tau^2/2\sigma_\tau^2}} \tag{6}$$

with $\sigma_\tau = 0.2\sigma$ and expectation value

$$\langle \tau \rangle = \tau_0 + \sum_{\tau=\tau_{\min}}^{\tau_{\max}} \tau \times f_{\text{ring}}(\tau)\,. \tag{7}$$

For our choice of parameters (N=200, v_c=0.2 m/s [Bartos et al., 2002, Strüber et al., 2017], τ_0=0.5 ms) the delays in the network varied between 0.7 ms and 10.5 ms in steps of 0.2 ms, yielding an average $\langle \tau \rangle \approx 4.1$ ms.

If all neurons spike synchronously, and taking into account the multiplicity of synapses per connection n_{syn}, we thus expect a compound inhibitory conductance time course (see Fig. 1D)

$$G_{\text{syn,GABA}}(t) = 2\sum_{\tau=\tau_{\min}}^{\tau_{\max}} e^{\tau^2/2\sigma_\tau^2} \lfloor n_{\max} e^{\tau^2/2\sigma_\tau^2} \rfloor g_{\text{syn,GABA}}(t-\tau)\,. \tag{8}$$

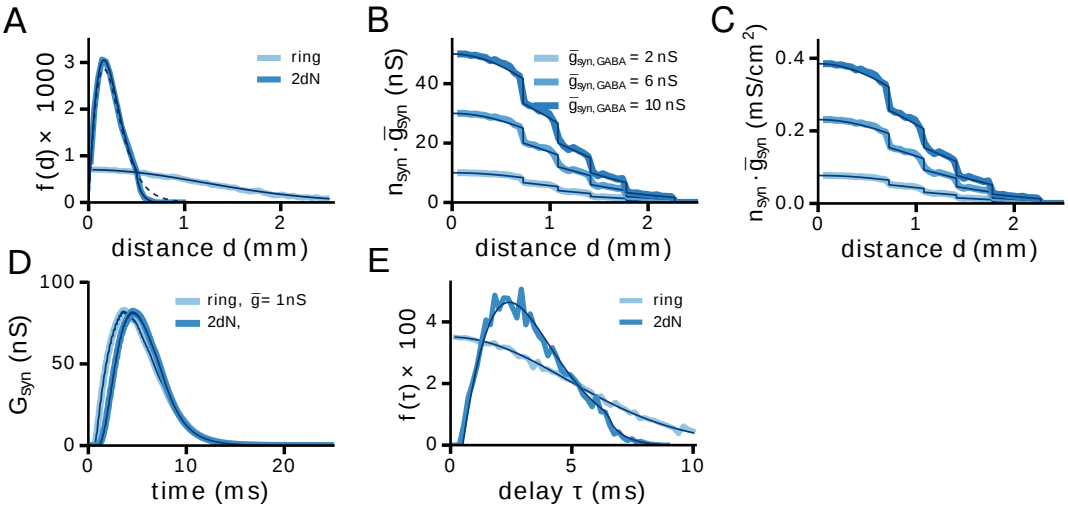

Figure 1: **Connectivity statistics (A)** Density function of distances $f(d)$ for the ring network (light blue) and the network embedded in two-dimensional space (darker blue) as estimated from a network instantiation versus the theoretical prediction (thin dark blue lines). For the two-dimensional (2dN) network we also show $f(d)$ for the network without a maximal distance of L=1 mm (dashed line, see text). **(B)** Unitary, i.e., total inhibitory synaptic conductance between two PV cells at distance d for three different individual synaptic peak conductances $\bar{g}_{syn}$. **(C)** Same as (B) in terms of the specific conductance, i.e., normalized by the cell area. Dark blue lines are respective analytical expectations. **(D)** Total inhibitory conductance received by a PV cell from all presynaptic cells assuming full synchrony for the ring network and peak conductance $\bar{g}_{syn}$=1 nS ($\approx 0.008\,\mathrm{mS/cm^2}$) (light blue). The two-dimensional network was fitted to obtain a similar G_{syn} (dark blue, parameters $\tau_{2dN}(d) = \tau_0$+12s/m $\times$ d and $n_{syn,2dN}$=7). **(E)** The respective delay distributions for ring and 2d-network after fitting $G_{syn,rand}$. Wide lines in (D,E) are as measured from a network instantiations, dark blue lines are analytical expectations.

Two-dimensional networks

To avoid boundary effects, we embedded N neurons in a two-dimensional torus of size $L \times L$. Neuron positions were chosen uniform-randomly. Networks were created following the spatial connection probability of PV basket cells measured in [Espinoza et al., 2018]. In particular,

$$p_{2\mathrm{dN}}(d) = \frac{1}{1+\exp\left(\frac{d-a}{b}\right)}\,\Theta[L/\sqrt{2}-d]\,. \tag{9}$$

The expected number of connections per cell is then given by

$$\langle k_{2\mathrm{dN}}\rangle = \int_{d_{\min}}^{d_{\max}} \rho_{2\mathrm{dN}}(x)p_{2\mathrm{dN}}(x)\,dx = \int_{0}^{L/\sqrt{2}} \frac{\rho_{2\mathrm{dN}}(x)}{1+\exp\left(\frac{d-a}{b}\right)}\,dx \tag{10}$$

with cell density at a given distance d given by (assuming homogeneous cell density $2N/L^2$)

$$\rho_{2\mathrm{dN}}(d) = \begin{cases} \frac{2N\pi d}{L^2} & \text{for } 0 \le d \le L/2 \\ \frac{2Nd}{L^2}\left(\pi - 4\arccos\left(L/2d\right)\right) & \text{for } L/2 < d \le L/\sqrt{2} \\ 0 & \text{otherwise}\,. \end{cases} \tag{11}$$

The cases in Eqn. (11) arise from the necessity to avoid ambiguity on a torus due to overlap. The connection probability $p_{2\mathrm{dN}}(d)$ is small for d >500 µm, so we chose a layer size L=1 000 µm for which Eqn. 11 is well approximated by $2N\pi d/L^2$ (Fig. 1A, solid vs. dashed line). The expected number of connected neurons is then given by $\langle k_{2\mathrm{dN}}\rangle \approx 0.097N$. To match $\langle k_{\mathrm{ring}}\rangle$=58 we would need N=600 cells in the 2d-network, which proved computationally difficult. We thus chose N=300 and increased the number of synapses $n_{\mathrm{syn,2dN}}$ per connected pair to compensate for the missing connections.

In order to constrain the conduction velocity $v_{c,\mathrm{2dN}}$ and $n_{\mathrm{syn,2dN}}$, we matched the compound synchronous inhibitory conductance $G_{\mathrm{syn,2dN}}(t)$ to the one expected for ring networks, see Eqn. (8) and Fig. 1D. Due to the linear increase in the number of cells at a given distance it follows that there are only few cells at very short distances, explaining the shift of $G_{\mathrm{syn,2dN}}(t)$ towards later times compared to $G_{\mathrm{syn,ring}}(t)$. We found that otherwise a good fit is established for $\tau_{2\mathrm{dN}}(d)$=12s/m $\times$ d (i.e. a three times smaller conduction velocity $v_{c,\mathrm{2dN}}$=0.0833 m/s than for ring networks) and $n_{\mathrm{syn,2dN}}$=7 (independent of distance, for sake of simplicity), see Fig. 1E. The respective delay distribution $f(\tau)$ is a rescaled version of $f(d)$ with mean delay $\langle\tau_{2\mathrm{dN}}\rangle \approx 3.3$ ms (shown for comparison in Fig. 1E).

Synchrony Index and Coherence

In several key studies [Bartos et al., 2002, Wang and Buzsáki, 1996, Bartos et al., 2001, Vida et al., 2006] a coherence-based measure was used to quantify synchrony in a network. In particular,

$$\kappa = \frac{2}{N(N-1)}\sum_{i=1}^{N}\sum_{j=i+1}^{N}\kappa_{ij} \tag{12}$$

$$\text{with}\quad \kappa_{ij}(\Delta) = \frac{\sum_{k=1}^{K} X_i(k)X_j(k)}{\sqrt{\sum_{k=1}^{K} X_i(k)\sum_{k=1}^{K} X_j(k)}}\,,$$

$$\text{where if}\quad X_i(k)X_j(k) > 1: \quad X_i(k)X_j(k) = 1$$

with binsize Δ, spike count histogram $X_i = \text{hist}[S_i(t)|\Delta]$ and number of bins $K = \left\lceil \frac{T}{\Delta} \right\rceil$ for considered time interval T. In the coherence measure employed in [Bartos et al., 2002, Bartos et al., 2001, Vida et al., 2006] the bin size is, moreover, adapted to the network firing rate r as $\Delta(r)$=0.1/r. We find that the Synchrony Index FF/N as a global population activity-based measure is much simpler to quantify oscillatory behavior. The coherence measure potentially ignores spikes (it sets presence of any number of spikes per bin per neuron to one, see Eqn. (12)) and can also be high for non-oscillatory states, e.g., travelling waves. For the regimes we were considering, we found that the coherence measure κ also produces a floor at low or no synchrony (see Fig. **??**B, 2D), which the FF-based Synchrony Index does not show. The FF on the other hand needs a very small time bin (smaller or equal to the sampling time) to correctly estimate FF=N for perfect synchrony (Fig. 2A), which for Poisson process driven neuron actvity is never quite the case. We optimized the time bin to yield maximal FF for a wide range of synchrony, see light blue solid curves in Fig. 2.

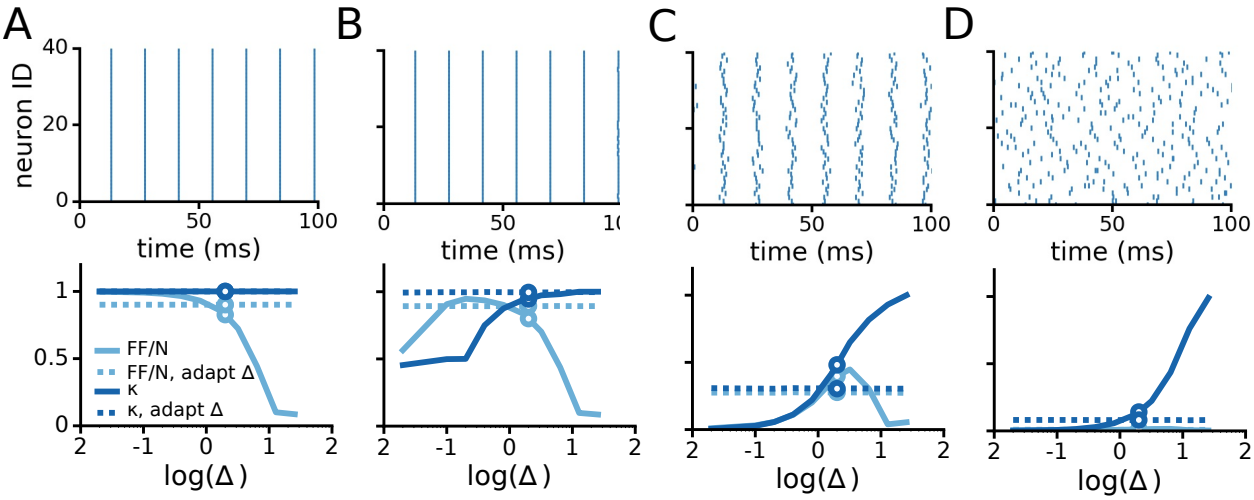

Figure 2: **Fano-factor-based Synchrony index vs. Coherence Measure (A-D)** Upper row: Different variations of synchrony measures: Synchrony Index FF/N as function of fixed bin size (solid light blue), FF/N for adaptive bin size, i.e. dependent on the inverse of the firing rate (dashed light blue, firing rate is constant across panels at 70 Hz), coherence κ as function of bin size ([Wang and Buzsáki, 1996], solid dark blue, see Eqn. (12)), and κ for adaptive bin size ([Bartos et al., 2002, Bartos et al., 2001, Vida et al., 2006], dashed dark blue). Circle: δ=2 ms is the value we consistently used to compute the synchrony index in our results. Lower row: respective spike data used to compute FF/N and κ. We used surrogate data, i.e., N=40 copies of the same regular spike train with increasing normally distributed jitter with standard deviation σ. (A) σ=0 ms, (B) σ=0.1 ms, (C) σ=10 ms, (D) σ=50 ms.

References

[Bartos et al., 2001] Bartos, M., Vida, I., Frotscher, M., Geiger, J. R. P., and Jonas, P. (2001). Rapid signaling at inhibitory synapses in a dentate gyrus interneuron network. *Journal of Neuroscience*, 21(8):2687–2698.

[Bartos et al., 2002] Bartos, M., Vida, I., Frotscher, M., Meyer, A., Monyer, H., Geiger, J. R. P., and Jonas, P. (2002). Fast synaptic inhibition promotes synchronized gamma oscillations in hippocampal interneuron networks. *Proceedings of the National Academy of Sciences*, 99(20):13222–13227.

[Espinoza et al., 2018] Espinoza, C., Guzman, S. J., Zhang, X., and Jonas, P. (2018). Parvalbumin+ interneurons obey unique connectivity rules and establish a powerful lateral-inhibition microcircuit in dentate gyrus. *Nature Communications*, 9(1):4605.

[Strüber et al., 2017] Strüber, M., Sauer, J.-F., Jonas, P., and Bartos, M. (2017). Strength and duration of perisomatic gabaergic inhibition depend on distance between synaptically connected cells. *Proceedings of the National Academy of Sciences*, 8:758.

[Vida et al., 2006] Vida, I., Bartos, M., and Jonas, P. (2006). Shunting inhibition improves robustness of gamma oscillations in hippocampal interneuron networks by homogenizing firing rates. *Neuron*, 49(1):107 – 117.

[Wang and Buzsáki, 1996] Wang, X.-J. and Buzsáki, G. (1996). Gamma oscillation by synaptic inhibition in a hippocampal interneuronal network model. *Journal of Neuroscience*, 16(20):6402–6413.